KERNFORSCHUNGSZENTRUM

KARLSRUHE

März 1973 KFK 1782

Institut für Angewandte Systemtechnik und Reaktorphysik
Projekt Schneller Brüter

Preliminary Analysis of the Predisassembly Phase of the Unprotected Overpower Transient Accident for SNR 300

W. E. Kastenberg, E. T. Rumble

GESELLSCHAFT
FÜR
KERNFORSCHUNG M.B.H.

KARLSRUHE

GESELLSCHAFT FÜR KERNFORSCHUNG M. B. H.
KARLSRUHE

KERNFORSCHUNGSZENTRUM KARLSRUHE

KFK-1782

Institut für Angewandte Systemtechnik und Reaktorphysik

Projekt Schneller Brüter

PRELIMINARY ANALYSIS OF THE PREDISASSEMBLY PHASE OF THE UNPROTECTED OVERPOWER TRANSIENT ACCIDENT FOR SNR 300

William E. Kastenberg*

Edmund T. Rumble III**

* Guest Scientist from the University of California, Los Angeles, California, USA

** Guest Student from the University of California, Los Angeles, California, USA

Gesellschaft für Kernforschung m.b.H., Karlsruhe

ZUSAMMENFASSUNG

Ein vereinfachtes Modell der Predisassembly-Phase für unkontrollierbare Überleistungstransienten in LMFBR wird erläutert. Das Modell berücksichtigt die Wechselwirkung zwischen geschmolzenem Brennstoff und Kühlmittel im Kühlkanal und die daraus resultierende Brennstoffbewegung und Na-Ausstoßung. SNR-300 wird analysiert und die Ergebnisse werden mit den Ergebnissen der SAS-VENUS-Rechnungen verglichen, in welchen Brennstoffbewegungen nicht berücksichtigt werden. Die Ergebnisse zeigen, daß das Ausmaß des Transienten, soweit er von der integrierten thermischen Energie, der Temperatur und des geschmolzenen Brennstoffs abhängt, wesentlich reduziert werden kann, wenn die Brennstoffbewegung berücksichtigt wird.

ABSTRACT

A simplified model of the predisassembly phase for unprotected overpower transients in LMFBR's is presented. The model includes fuel movement and sodium expulsion as a result of the molten fuel-coolant thermal interaction in the channels. The SNR-300, a prototype/demonstration plant is analysed and the results compared to an earlier set of calculations using the SAS-VENUS computational models. The previous analysis neglects fuel movement. The results indicate that substantial reductions in the severity of the transient, as measured by molten fuel produced, the thermal energy generated, and the final temperatures, can be obtained when fuel movement is included.

Contents

I. INTRODUCTION

Despite the multitude of redundant and diverse trips designed to ensure the safe and reliable operation of SNR 3oo, the analysis of hypothetical accidents is still important in the design of the pressure vessel, containment and in licencing /1/. The unprotected overpower transient ie; addition of positive reactivity accompanied by a failure of the primary and secondary shut down systems, requires further investigation because at present, it yields the highest work-energy available to damage the reactor structures. The analysis performed to date has been overly pessimistic because the reactivity feedback due to fuel movement, following the molten UO_2-Na interaction in the predisassembly phase, has been neglected /1/.

Mills and Kastenberg /2/ and Lorenzini and Flanagan /3/ were first to show that fuel motion during this phase of an accident could lead to shut down of the reactor, even before gross disassembly accompanied by high pressures, high energy and high temperatures, can take place. The importance of this potential for lowering the work-energy has stimulated further research as reported at the recent meeting on safety at Karlsruhe /4,6,7/.

The object of this report is to:

1) analyse the SNR-3oo design using a simple model, which includes fuel feedback, developed at UCLA /4,5/,
2) compare these new results with those obtained for SNR-3oo using the SAS-VENUS code modules at Argonne (which do not include fuel movement) /1,6/ and
3) discuss those areas in this simple model which require improvement and modification, so that a more realistic picture of the physics and hence the work-energy can be obtained.

These objectives serve as justification and underscore the importance, of future work in this area.

One point that should be made here (and again in the conclusions) is that without fuel movement, the conservative approach is generally the one that gives the highest pressures and subsequently the highest positive ramps due to sodium expulsion during the transition to disassembly. With fuel movement, this is not always the case since faster sodium expulsion also means faster fuel movement. Since the problem is nonlinear,and depends on a variety of parameters (fuel particle size, drag coefficients, failure thresholds etc) it is not always clear that the most pessimistic assumptions without fuel movement are those when fuel movement is included. This point will be discussed again.

II. PHYSICAL MODEL

The unprotected over power transient is assumed to be initiated by a reactivity ramp of several to a few tens of dollars per second. The primary and secondary shut down systems are assumed to fail and the power increases, accompanied by a steep increase in fuel temperature. This occurs in 1oo to 3oo milliseconds. The doppler feedback, generated by the fuel temperature increase, keeps the reactivity below prompt critical. At this point the central portion of the fuel pins in the inner regions of the core begin to melt with subsequent failure of the fuel pins due to fuel vapor pressure (as in the case of new pins) or retained fission gas pressure (as in the case of highly irradiated pins). This pressure also drives the molten fuel into the coolant channel and a fuel-coolant interaction ensues. There is an immediate rise in the ramp insertion of reactivity caused by a reverse doppler effect due to fuel chilling and by the rise of pressure causing sodium ejection. The reactor may then go slightly super prompt critical causing more melting of the core with failure of fuel and subsequent thermal interactions. After several milliseconds however, the fuel in the channels where failure has occurred will also be ejected due to drag forces on the particles. This results in a sharp decrease in the ramp rate. If enough fuel is moved, the ramp becomes negative, resulting ultimately in termination or shut down of the transient.

The computer module employed in this study contains a neutronics and a hydrodynamics model. For this study, the point kinetics model with six groups of delayed neutrons, based on the forward march technique of Hanson was used for the neutronics /8/. The core is divided into M axial and K radial regions and the doppler feedback is calculated by

$$\Delta \rho_{\text{Doppler}} = - \alpha \sum_{m=1}^{M} \sum_{k=1}^{K} \alpha_{m,k} \ln \left(\frac{T_{m,k}}{T^{o}_{m,k}} \right) \qquad (1)$$

where α is the overall doppler coefficient for the reactor, $\alpha_{m,k}$ is the volume weighted doppler worth of region m,k, $T_{m,k}$ is the temperature of region m,k and $T^{o}_{m,k}$ is the initial temperature of region m,k. The coolant temperature is considered constant until the fuel-coolant interaction takes place and the transient is assumed adiabatic. Hence $T_{m,k}$ (t) is obtained from

$$T_{m,k}(t) = T^{o}_{m,k} + \gamma^{o}_{m,k} \int_{o}^{t} P(t')\, dt' \qquad (2)$$

where P (t) is the power at time t, $\gamma^{o}_{m,k}$ is the volume weighted power shape and the superscript (o) refers to the initial temperature. Each region is characterized by an average fuel temperature and failure is initiated when this average temperature reaches a certain threshold. Independent calculations /9/ show that when 5o% of the areal midplane is molten, the average temperature of the midplane is between 29oo^{o}K and 32oo^{o}K while the average temperature of only the molten part is between 3o4o^{o}K and 33oo^{o}K depending on the pin characteristics. Since the mechanisms for failure are not well understood, an amount between 4o and 6o percent is generally used as the criterion for failure /1,5,6/ and is varied to test for sensitivity. For the model used here, only a threshold temperature can be specified and is varied between 3o41^{o}K and 3241^{o}K. In addition it is assumed that the failure only occurs in the center node (at the axial midplane) where the power is highest.

After pin failure, the thermal interaction is modeled as follows. The fuel-coolant mixture is characterized by T_{Mix}, the mixture temperature computed from:

$$T_{Mix} = T_o + (T_f - T_o) \quad (1-e^{-\lambda t}) \qquad (3)$$

where

T_o = initial sodium temperature

T_f = final sodium temperature assuming instantaneous mixing and a constant volume process

λ = input parameter depending on particle size

The input parameter λ allows one to match various heat transfer models /3,4,5/ and various particle sizes /3/. This increase in temperature in the interacting volume results in pressure generation given by the sodium equations of state. Inside the two-phase region the pressure is calculated by

$$\log_e P = a - \frac{b}{T} - \frac{c}{T_2} + dT - e \log_e T \qquad (4)$$

and outside the vapor dome by the Himpan equation of state

$$\left[P + \frac{a}{(v-b)(Tv-c)} \right] (v-d) = RT \qquad (5)$$

The constants are given in the Appendix.

Under the influence of this pressure, the interacting volume is assumed to expand symmetrically about the axial midplane. The sodium displacement is determined by

$$F_z = \frac{m dV_c}{dt} \qquad (6)$$

where m is the mass of the sodium column above the interacting zone and $V_c(t)$ is the velocity. The forces are the pressure and gravity. The interfacial movement is then determined from the velocity. It is also assumed that the initial sodium velocity is zero and that only the fuel in the axial midplane node interacts. This is consistant with the symmetry picture.

The drag force on the fuel particles is given by:

$$F_D = \frac{1}{2} \frac{\pi D_p^2}{4} (V_p - V_c)^2 C_D \rho \qquad (7)$$

where:

D_p = particle diameter
ρ = sodium density
V_p = particle velocity
V_c = sodium velocity
C_D = drag coefficient.

The drag coefficient is chosen to be o.44 /3/. The displacement, as in the case of sodium, is calculated from an integration of Equation (6).

The feedback due to fuel and sodium movement are obtained from worth curves. Perturbation or eigenvalue calculations may be used and differential worths converted to a cubic or quartic polynomial. The reactivity calculation is different for fuel and sodium. For fuel, it is assumed that the mixed fuel is spread uniformly through the channel as the interface moves up (and down) increasing the size of the interacting volume. Hence there is loss of reactivity as some fuel moves to regions of lower worth. For sodium, the column moves up and origional coolant is replaced by coolant of reduced density. Consistant with perturbation theory, it is assumed that the reactivity worth varies linearly with changes in density. Hence the reactivity change associated with the fuel in one region is half, if only half the fuel moves out of that region.

The SAS-VENUS modules depict the same series of events in a similiar way with the following major exceptions. After the fuel-coolant interaction takes place in a channel, only the positive void rate in SAS, was accounted for. Also, when the fuel vapor pressures begin to build up, a switch from SAS to VENUS is made. This switch is characterized by an increased ramp rate (transitional ramp) and shut down is achieved via a Bethe-Tait type analysis. Other differences are discussed in reference /1/.

III SNR-3oo DATA

The SNR-3oo LMFBR was analysed with the computational model outlined above. The core was divided into 1o radial and 18 axial regions as was done in the previous SNR-3oo analysis /1o/. Similiary, the significant neutronic data (neutron life time, doppler coefficient, delayed neutron fractions, etc.), the doppler worths, fuel worths, sodium worths, initial temperature distribution, power shape and fuel and sodium mass fractions were obtained from reference /1o/. One major difference is the thermodynamic data used. The model employed in this study uses only average values of the various specific heats while the previous calculations use tabulations to account for temperature dependence. The significant thermodynamic data employed is given in the Appendix.

Another difference is that the axial molten zone for the thermal interaction in the SAS-VENUS calculation was 3o cm. Since the model used here can only have failure in the center node, we obtain an interaction zone of 2o cm (approximately). The fuel sodium interaction is equivalent since the mass ratios of fuel and coolant stay the same. However, this makes the present calculation conservative because less fuel is moved out as compared to the SAS-VENUS runs. If we artificially increase the amount of fuel and sodium, taking place in the interaction, the negative feedback is to strong because it will come from the highest worth regions rather than be spread out over a larger worth region.

One interesting feature of the SNR-3oo fuel worth curves are that the maximum values are below the axial midplane, while the temperature peaks at the midplane or the axial node above the midplane. Since the model only treats the case of midplane failure, there is an initial positive contribution for fuel movement as the fuel particles move down the channel. This effect is included in the results presented and occurs because of the difference in the top and bottom reflectors.

IV. SNR-300 ANALYSIS

For the nominal case, the reactivity ramp is taken as $ 5/sec., the fuel particle size is 300 μ diameter (150 μ radius), 50% of the radial pin cross section is molten and 100% of the molten fuel participates in the fuel coolant interaction. In addition the failure threshold is taken to be 3141°K. Since this is the only average temperature calculated for the central node, the molten fuel participating in the fuel-coolant interaction is also at 3141°K. Cases at 3041°K and 3241°K were also run and are discussed below.A drag coefficient C_D = 0.44 was also chosen since it represents the theoretical lower limit and appears valid in the sodium velocity range of interest. Higher values yield a higher drage force which results in quicker movement of fuel. Hence we have taken the most conservative approach here.

The transient proceeds as described in Section II and compares with the SAS-VENUS result up to the initiation of failure. As shown in Figure 1, the power reaches 40 times the nominal power in 350 milliseconds. The average temperature in the central axial node is 3141°K (100°K above the melting point) over a 20 cm axial length. This assumes that 50% of the areal cross section is molten.

At 352 milliseconds the pins fail in the first region followed by those in the second at 355 milliseconds and those in the third at 360 milliseconds. During this time period the power rises sharply due to the increased ramp rate caused by sodium expulsion. At 360 milliseconds, a large negative contribution comes into play caused by the fuel movement and the transient is terminated (defined when P/P_0 = 0.95) abruptly. The reactivity components are shown in Figure 2. Note that the net reactivity hovers below prompt critical until the sodium moves out and superprompt criticality is maintained for only about 5 milliseconds.

Table I shows a comparison of this case with the failure thresholds of 3041°K and 3241°K.

Table I Sensitivity to failure threshold for $ 5/sec ramp, 15o/u fuel particle and 5o% of fuel pin (1oo% of molten fuel) taking part in the thermal interaction.

failure threshold	3o41°K	3141°K	3241°K
+ thermal energy release (MWsec)	154	337	425
ave.temp. of molten fuel (°K)	3o65	3133	3152
amount of molten fuel(kg)	524	1o2o	1248

+ In this and following tables, the energy released is that stored in the molten fuel only and includes the heat of fusion.

Table I shows that when the fuel failure threshold is increased, the energy yield, average temperature of the molten fuel and the amount will increase. The increased threshold for failure delays the fuel movement, permits more positive reactivity to be inserted, requires more movement for shut down and therefore increases the yield. The increased molten fuel temperature also enhances the fuel-coolant interaction, driving the fuel and sodium out quicker but since the problem is nonlinear, this latter effect is not as important for the slow ramps of $ 5/sec.

In Table II, the effect of particle size on the transient is shown.

Table II. Effect of particle size on the nominal case with 5o% of cross section molten and 1oo% of the melt taking part in the thermal interaction.

Threshold	3o41°K	3141°K	3241°K
5o/u (radius)	14o MWsec 3o61°K 48o kg	337 MWsec 3133°K 1o2o kg	425 MWsec 3151°K 1248 kg
15o/u(radius)	154 MWsec 3o65°K 524 kg	337 MWsec 3133°K 1o2o kg	425 MWsec 3152°K 1248 kg
3oo/u(radius)	287 MWsec 3117°K 892 kg	364 MWsec 3139°K 1o9o kg	358 MWsec 3135°K 1o77 kg

In general, increasing the particle size tends to increase the energy in the molten fuel, the amount of molten fuel and its temperature. However, there are two competing processes; the positive ramps due to the insertion and the sodium, and the negative ramp due to fuel. Their time sequencing is sensitive to the particle size because of drag, heat transfer and pressure generation. In the 3241^{o}K threshold case, the failure and subsequent thermal interaction are held back in time so that more fuel movement is needed to overcome the $ 5 sec ramp insertion even though the fuel moves quicker for the 50μ radius fuel particle. For the general trend, the fuel-coolant interaction and the motion due to the drag force is smaller with increased particle size. This tends to incerease the amount of total molten fuel and its energy and temperature.

There are three cases analysed with the SAS-VENUS code, neglecting fuel feedback, which can be used for comparison of the $ 5/sec ramp. These are for the case of 150μ fuel particle radius and

a) 45% molten areal cross section molten/100% of molten fuel participating in the fuel coolant interaction,

b) 60% molten areal cross section molten/100% of molten fuel participating in the fuel coolant interaction,

c) 60% molten areal cross section molten/50% of molten fuel participating in the fuel-coolant interaction.

Case a) gives the highest energy yield because the low failure criterion (45% areal cross section molten) permits more channels to fail which in turn produces a higher ramp rate (due to sodium voiding) in the transition to disassembly. Case b) produce a smaller yield, even though the amount of fuel/pin taking place in the thermal interaction is larger, producing faster sodium movement, the total movement is less because high fuel vapor pressures are reached before the number of failures of case a) is reached and the transition to disassembly takes place. Case c) produces the weakest accident because both the amount of fuel/pin and fuel/core taking place in the thermal interaction is smaller.

Table III shows a comparison of the worst case for the SAS-VENUS modules (case (a) above), with the only difference being the size of the interacting zone as discussed previously.

Table III. Comparison of $ 5/sec ramp with and without fuel feedback for 15o/u radius fuel particle, 45% of areal cross section molten and 1oo% of molten fuel taking part in thermal interaction.

	without feedback /1/	with feedback		
		3o41°K	3141°K	3241°K
thermal energy released (MWsec)	2o8o	589	667	896
average temp. of molten fuel (°K)	3756	3214	3247	333o
amount of molten fuel (kg)	2515	1569	1697	2o43

The pessimistic nature of neglecting the feedback due to fuel movement becomes obvious when examining Tables I-III above. The 45% threshold in SAS-VENUS correspond to an early pin failure, with a lower molten fuel temperature. Hence, the case of 3o41°K is probably the closest for comparison purposes. The energy yield is reduced by a factor of 4, the amount of molten fuel is nearly one half and the final temperature of the melt is reduced 5oo°K when fuel movement is included. The results are conservative because of the smaller axial molten zone and because the SAS-VENUS results only give the energy generated during the disassembly stage.

A comparison of the cases a), b) and c) with equivalent cases including fuel movement are shown in Table IV.

Table IV Comparison of accident spectrum for 150 μ particle radius and $ 5/sec ramp with and without fuel movement.[+]

Fraction of total fuel leaving pin	0.250			0.450			0.600			case (a)	case (b)	case (c)
Threshold temperature for failure (^{0}K)	3041	3141	3241	3041	3141	3241	3041	3141	3241	-	-	-
Thermal Energy Released (MWsec)	all pins fail			589	667	896	257	243	1050	2080	1980	1760
Amount of Molten Fuel (kg)	whole core melts without shut down			1569	1697	2043	799	1051	2516	2515	1372	946
Ave.Temperature of Molten Fuel (^{0}K)	$3550 < T < T_{VAPOR}$			3214	3247	3330	3102	3123	3297	3756	3200	3140

[+]
case (a) is equivalent to 0.450
case (b) is equivalent to 0.600
case (c) is equivalent to 0.250

Table VII permits us to make the following comparisons. Case (a),as we have seen,corresponds to the case of o.45 fuel fraction and the 3o41^{o}K failure threshold. For the SAS-VENUS case (b), the failure threshold is delayed,hence there is more molten fuel per pin and it is hotter. This would compare to the case of o.6o fuel fraction and 3141^{o}K. In both cases the accident gets weaker and in the same proportion. If we examine case (c), where only 5o% of the molten fuel mixes with coolant, we have a high threshold and its comparison is the case of o.25o fraction and threshold temperature of 3241^{o}K. Here the model with fuel movement breaks down because the fuel vaporizes before shutdown. The code should be stopped and the switch to a VENUS type disassembly should be made. In such a case, the transition ramp rate will be smaller and the result will compare favorably with case (c).

One must be carefull when drawing conclusions because the calculations are sensitive to the threshold used (either temperature or fraction of molten fuel), particle size and the amount of fuel taking part in the fuel coolant interaction.

An example of this sensitivity is the case of the 3241^{o}K failure threshold with 6o% and 5o% areal fractions of molten fuel (Tables I and IV). Increasing the amount of fuel 2o% yields a 1oo% increase in thermal energy released, and doubles the amount of molten fuel. Examination of the reactivity calculation shows that it reaches prompt critical as in the other cases, but now, since there is a little larger contribution of positive feedback due to the asymmetrical fuel worth curves (as discussed in Section III), the net reactivity oscialltes about prompt critical (β effective = o.3o4 x 1o^{-2}) as each region fails. This effect is most sensitive at high molten fuel temperatures where the thermal interaction is important. While 3241^{o}K is at the high end of the spectrum, it sill illustrates the point to be made concerning sensitivity.

Another example of this sensitivity can be seen by comparing the cases for 15o/u radius and fuel fractions o.45, o.5o and o.6o. As shown in Tables I and IV, the case with o.5o fuel fraction gives a milder accident for all fuel failure thresholds. There are competing processes; fuel movement (both positive and negative), heat transfer, sodium movement and drag. The overall trend is to lower the energy as the fuel fraction increases but there is a little oscillation in the curve at o.6o. This was observed previously for the 1,ooo MWe reactor analyzed by Mills and Kastenberg /4/. This is shown qualitatively in Figure 4 of the next section.

It is clearly evident that what is pessimistic for one case is not necessarily pessimistic for the other case. Hence one must be cautions when using the word pessimistic in describing approximations for the molten-fuel coolant interaction.

One other comparison that can be made is for the case of a $ 25/sec ramp. Two cases were calculated with the SAS-VENUS models and are compared with the model used here. The two SAS-VENUS runs corresponds to late and early failure of pins.

Table V. Comparison for $ 25/sec ramp with 15o/u radius fuel particle and 1oo% of molten fuel leaving pin.

	with fuel movement			without fuel movement /1/	
	3o41°K	3141°K	3241°K	late	early
thermal energy release (MWsec)	218o	2318	18oo	544	594
Mass of Molten Fuel (kg)	3654	3428	314o	124o	1324
Ave. temperature of molten fuel (°K)	3923	3768	3578	3o9o	325o

For this case, the model with fuel movement gives a larger yield then without fuel movement. This can be explained as follows. The axial model is for weak excursions. At $ 25/sec, examination of the temperature profile shows that much of the fuel is above 3691^{o}K in the nodes surrounding those that have failed before the fuel has begun to move up the channel. Hence the model is no longer applicable. Either one has to terminate the calculation earlier and proceede to a VENUS type analysis (since high fuel vapor pressures already exist) or one must modify the model to allow for fuel movement in other nodes. This will be explained in the next section.

IV FURTHER OBSERVATIONS

A general observation of the analysis for SNR-300 using SAS-VENUS is that the more total fuel participating in the molten fuel-coolant thermal interaction, the higher the transitional ramp rate and hence the thermal energy released. For the model trated here, the general trend is the opposite. Figure 3 shows a qualitative plot of energy released (at shut down) vs. fraction of total fuel participating in the thermal interaction. As the amount of fuel is reduced, both models should approach an asymptotic value. One can ask what this asymptotic value is. For the model used in this work, letting the fraction of fuel participating in the thermal interaction be reduced to zero, does not lead to a result because the core continues to get hotter without any shutdown mechanism. Physically, as this fuel fraction goes to zero, the core would vaporize in the center and shut down would occur due to vapor pressure. This energy could be obtained by running the SAS-VENUS code with only the $ 5/sec ramp and zero increase in transitional ramp rate.

Other usefull limiting cases are for zero particle size (instantaneous mixing with no time lag between fuel and sodium movement) and for very large particle size (where there is no heat transfer to sodium, no sodium void effect and the fuel is swept out due to drag forces exerted by the coolant flowing at a velocity of 5 meters/sec). Figure 4 shows these asymptotic results along with the values for 100, 300 and 600 μ diameter particles, and 50% fuel fraction (50% molten, 100% of molten fuel participating in the interaction).

For the case of the $ 5/sec ramp, with 5o% areal cross section molten and 1oo% of the molten fuel participating in the thermal interaction, the limiting cases yield an envelope for the thermal energy generated between 1oo MWsec and 6oo MWsec. This is for all particle sizes and all failure thresholds. For 6o% areal cross section molten and 1oo% of the molten fuel participating in the thermal interaction, all the points fall in this envelope except the high case of 3241°K threshold, as explained previously. For the case of 45% areal cross section molten, the consistant case of low temperature threshold, also falls within this envelope as well. For the high temperature threshold the energy is just outside the envelope (667 MWsec for 3141°K threshold) and below the extreme for the 6o% case (896 MWsec for the 3241°K threshold).

The conversion to usefull work for the SAS-VENUS worst case, (case a) yields approximately 2oo MWsec or a 1o% efficiency. With less molten fuel and at a lower temperature this efficiency should be less for the results reported here. Using the conservative approximation of 1o% efficiency on the nominal case; 15o/u particle radius, 5o% fuel fraction and 3141°K failure threshold yields a usefull work of 34 MWsec. Using this 1o% efficiency on the accident envelope above yields a spread of 14 MWsec to 6o MWsec.

VI NEED FOR FUTURE WORK

The present model is simple in many respects. At present it can only be used to show the importance of including fuel movement in unprotected overpower transients. There are several areas which need improvement.

The present model only allows fuel failure in the center node with instanteous mixing of fuel and coolant (but not heat transfer). A model which permits fuel movement within the pin and throughout the whole molten zone is required. In examining the results of the SNR-3oo analysis, the nodes surrounding those that fail usually become molten during the transient, and while they are counted in the total for molten fuel, they are not allowed to escape the pin. Some of this fuel will be ejected as it melts and should be accounted for. Walter /6/, argues that for slow transients (5o ¢/sec), failure of highly irradiated fuel will take place near the top of the core.

Hence molten fuel will be driven up the pin (while inside) by fission gas pressure and then out into the coolant channel. Hence the picture of fuel motion should be improved.

A second place where improvement is needed, is the fuel coolant thermal interaction. Mixing and fragmentation are assumed to occur instantaneously as opposed to heat transfer. For this analysis the approach may not be conservative since any delay will cause more fuel to become molten. However, there is also a delay in the increased positive ramp rate due to sodium ejection. Another feature is the calculation of the pressure generation as sodium heats up. The pressure calculated in the model, often reaches several thousand psi, much higher than observed in the TREAT tests /11/. One possible reason may be the condensation of sodium on the cold fuel and channel walls /11/. The simplified model used here needs improvement.

There are several programming limitations to the model used concerning heat genration in the mixed fuel after the fuel-coolant interaction, the doppler chilling, the average temperature used for both failure and fuel-coolant mixing and changing the doppler constant in regions where sodium is voided. These are felt to be second order effects when compared to the analysis discussed previously and can be considered as programming difficulties rather than physics difficulties.

VII CONCLUSIONS

The major conclusions that can be drawn from this analysis are as follows:

1) There is real incentive for correctly accounting for fuel movement in the predisassembly phase of unprotected overpower transients. Preliminary results show an order of magnitude reduction in thermal energy release and the amount of molten fuel is smaller and cooler then when movement is neglected.

2) Assumptions which make the results of the SAS-VENUS conservative do not in general make the results of this model conservative. In particular pessimistic assumptions regarding the molten fuel-sodium interaction tend to be reversed when including fuel movement.

3) Further analysis is required to establish a new, more realistic upper limit for the available work-energy on containment, vessel and structure. The present value appears to be pessimistic.

4) The results of this analysis should not be used for design studies because of the inherent limitations of the model.

5) Experimental evidence of the fuel movement should be obtained from inpile experiments with flowing sodium to verify the models developed.

Acknowledgement

The authors wish to thank Prof. Dr. Wolf Häfele for providing the creative atmosphere in which this work was accomplished and Drs. Kessler and Heusener for their enthausiasm for the work, providing the design and parametric data of SNR-300 and many usefull discussions.

REFERENCES

/1/ G. Heusener, G. Kessler, et.al. "Analysis of Hypothetical Accidents for SNR-300", Intern.Conference on Engineering of Fast Reactors for Safe and Reliable Operation.
Karlsruhe, Oct. 9-13, 1972

/2/ J. Mills and W.E. Kastenberg, "An Axial Kinetics Model for Fast Reactor Disassembly Accident," Proceedings of the Conference on New Developments in Reactor Math. & Appl.",
March 1971

/3/ P. Lorenzini and G. Flannagan, "Evaluation of Fuel-Coolant Interactions During Fast Reactor Disassembly", Proceedings of the Conference on New Developments in Reactor Math. & Appl.,
March 1971

/4/ J. Mills and W.E. Kastenberg, "The Evaluations of Fuel-Coolant Interactions on Kinetic During Fast Reactor Disassembly Accidents". Intern. Conf. on Engineering of Fast Reactors for Safe and Reliable Operation",
Karlsruhe 1972

/5/ S. Rowe, M.S. Thesis in Engineering, UCLA, unpublished

/6/ G.E. Culley, J.E. Hanson et. al. "Fast Reactor Safety Inplications of Recent Assessments of Fuel Pin Transient Behavior". Intern. Conference on Engineering of Fast Reactors for Safe and Reliable Operation",
Karlsruhe 1973

/7/ G.J. Fischer, W.R. Bohl, et. al. "Progress in the Analysis of Severe Accidents", Intern. Conf. on Engineering of Fast Reactors for Safe and Reliable Operation",
Karlsruhe 1972

/8/ K.F. Hansen et. al. "Stable Numerical Solutions to the Reactor Kinetic Equations", Nuc.Sci.Engr., 22, p 51. May 1965

/9/ J. Haun, M.S. Thesis in Engineering, UCLA, unpublished, June 1972

/10/ G. Heusener, G. Kessler, F. Dunn, J.Jackson, G.Fischer et. al. "Analysis of Hypothetical Accidents for SNR-300"
KFK-Report to be published

/11/ A.W. Cronenberg, H.K. Fauske and D.T. Eggen, "Analysis of the Coolant Behavior Following Fuel Failure and Molten UO_2-Na Interaction"
Nuc.Sci.Engr., Jan. 1973

APPENDIX

I. Physical and Thermodynamic Constants

	FUEL	SODIUM	UNITS
Specific heat of Solid	o.11	-	cal/gm-^{o}K
Specific heat of liquid	o.13	o.27	cal/gm-^{o}K
Heat of fusion	67	-	cal/gm.
Heat of vaporization	487	113o	cal/gm.
Melting temperature	3o4o	-	^{o}K
Vaporization temperature	3961	-	^{o}K
Sonic velocity	-	65oo	ft/sec
Critical Temperature	-	491o	^{o}R

II. Equation of State Constants[+]

$$P = \exp (a-b/T-c/T_2 + dT - e \ln T) \qquad (1)$$

Temperature Range

	a	b	c	d	e
below 2o43^{o}R	17.61o62	23,o73.3	o.o	o.oo	o.o5
2o43 to 2961^{o}R	18.432oo	22,982.o	o.o	o.o	o.63144
2961 to 491o^{o}R	1.77353	-12,61o.96	$3.4112 \times 1o^{-7}$	$1.12244o \times 1o^{-3}$	o.o

$$P = \frac{RT}{V-D} - \frac{A}{(V-B)(TV-C)} \qquad (2)$$

$A = 2.15982 \times 1o^{8}$ $\quad C = 255.6516$ $\quad R = 67.24859$

$B = 3.15937 \times 1o^{-4}$ $\quad D = 1.74661 \times 1o^{-2}$

+

In Equation (1) the pressure has units of pounds per square inch, temperature has units of degrees Rankine.

In Equation (2) the pressure has units of pounds per square foot, volume has the units of cubic feet per pound, and the temperature is expressed in degrees Rankine.

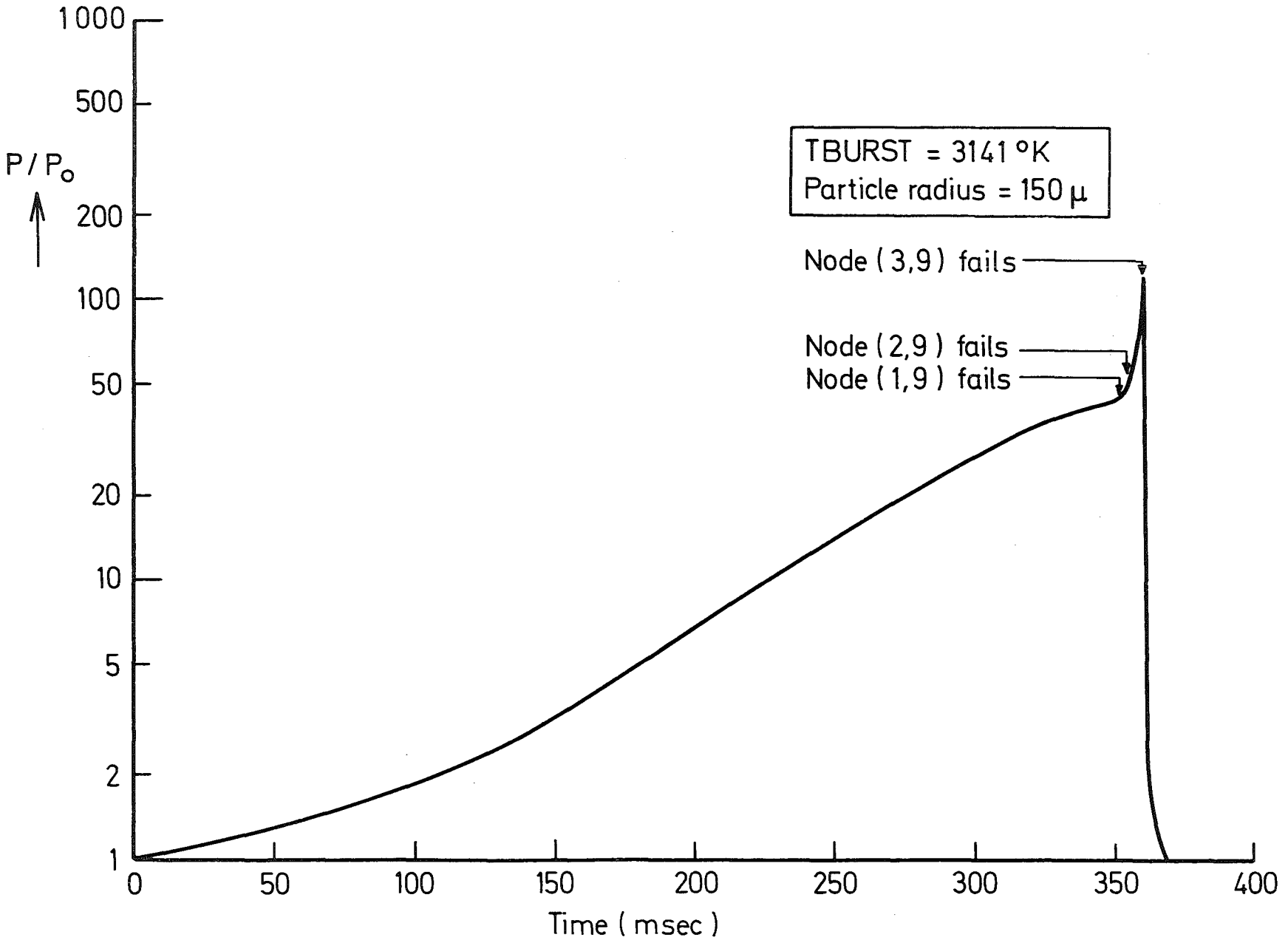

Fig. 1 Normalized reactor power versus time for \$5 / sec ramp

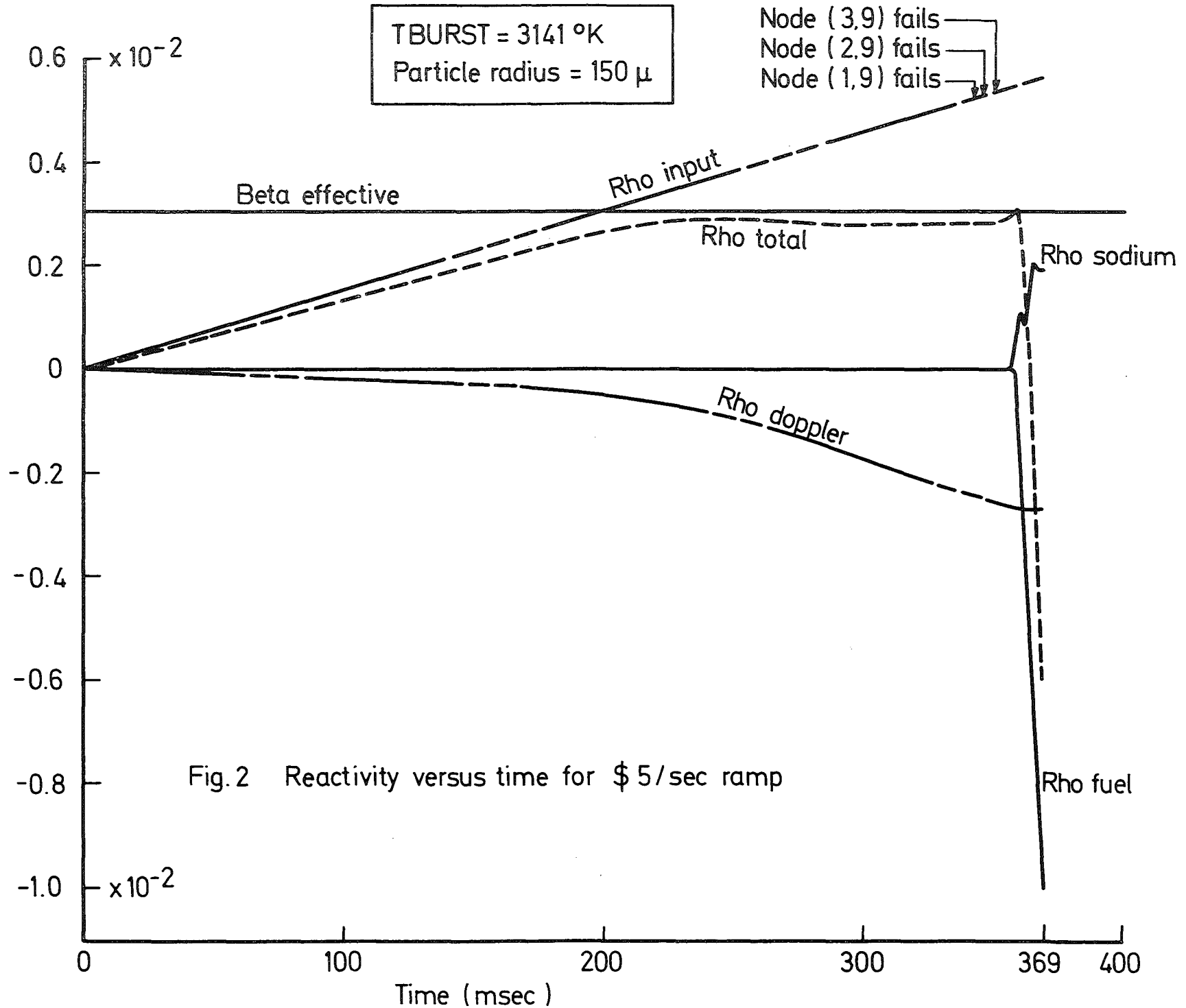

Fig. 2 Reactivity versus time for $ 5/sec ramp

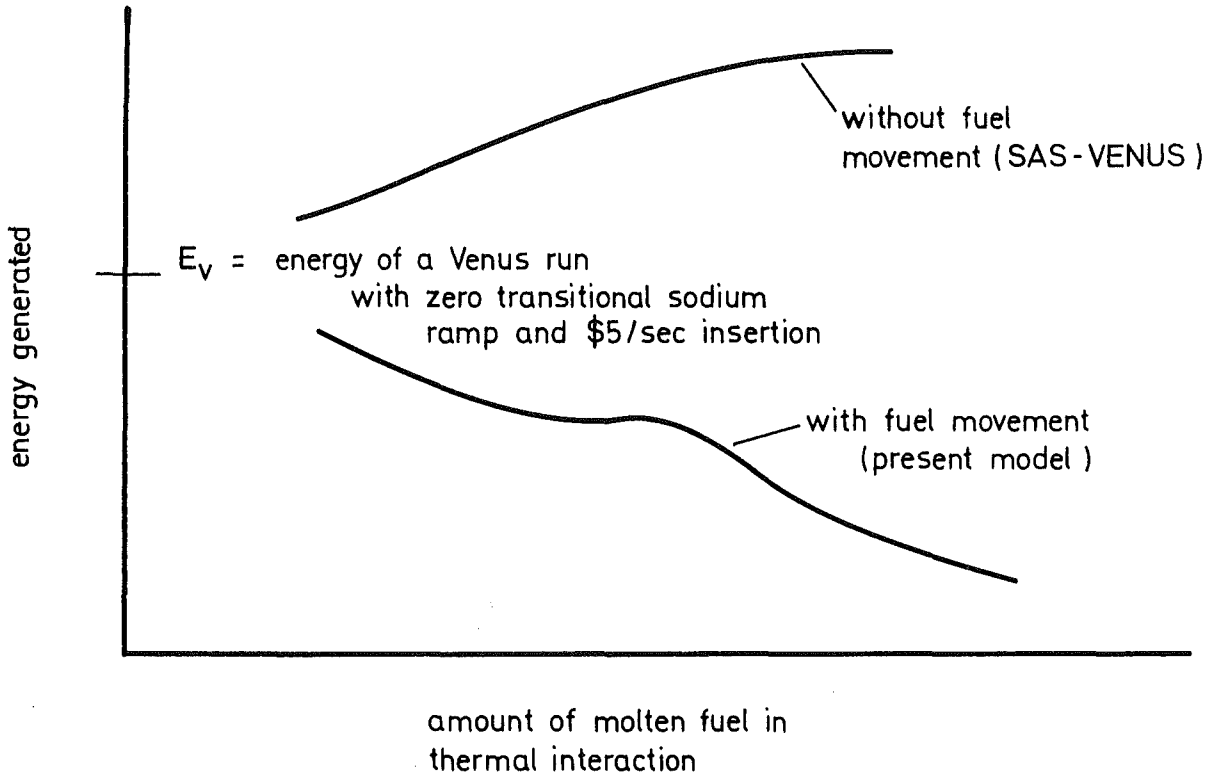

Fig. 3 Qualitative behavior of energy produced during unprotected overpower transient

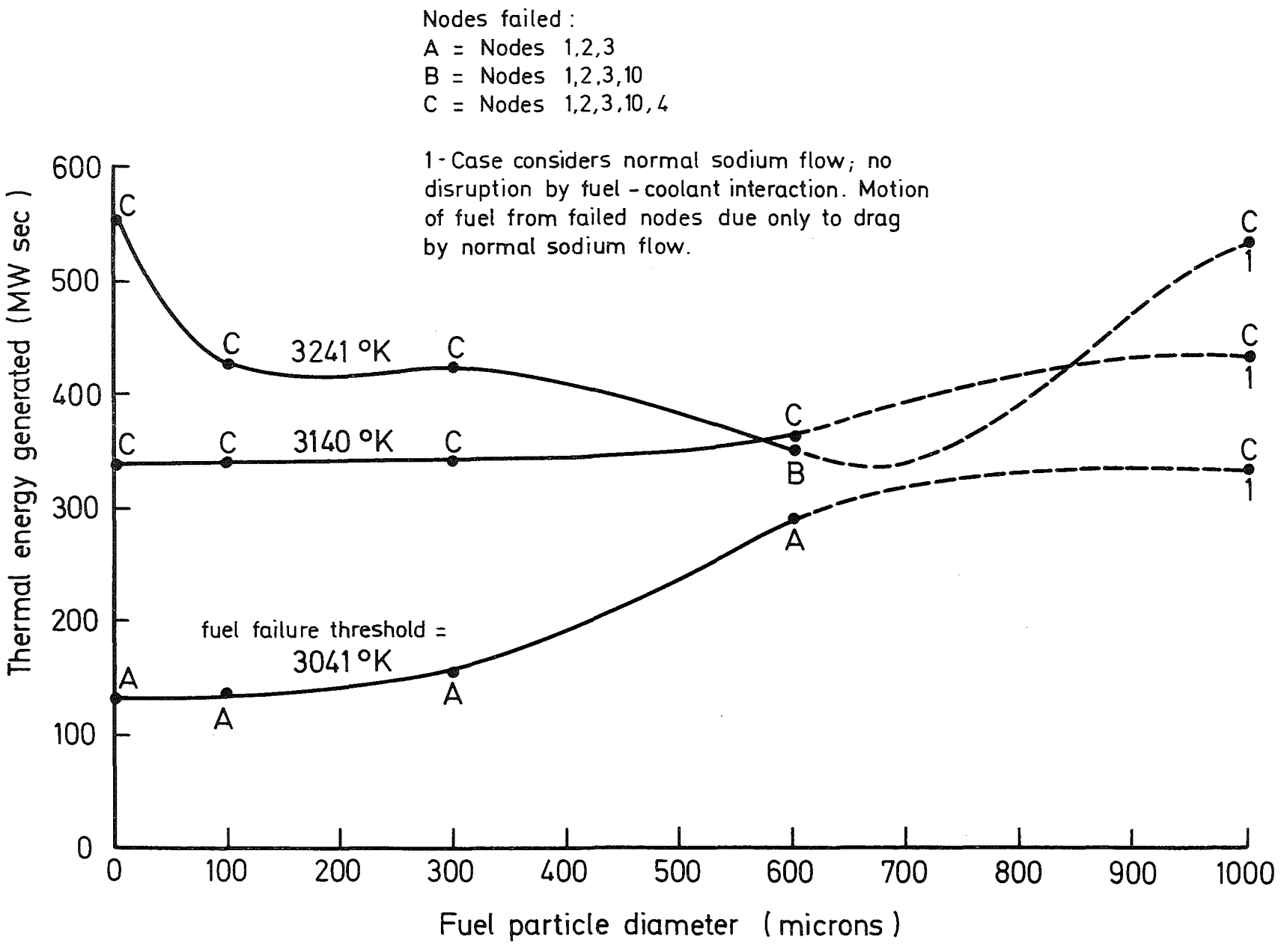

Fig. 4 Energy versus particle size